CHAPTER 4

RESULTS

LITHIUM NICKEL VANADATE BY THE SOL-GEL METHOD

4.1 Introduction

Lithium nickel vanadate, $LiNiVO_4$ is one of the promising cathode materials for lithium ion batteries. The high potential cell voltage is the reason why the compound has taken many interests from several researchers to study the performance of the cathode. Not to mention that this compound is the inverse spinel that was patented as potential cathode material and the first known Li intercalation reaction near 5 V for rechargeable Li cells.

In this chapter, the studies of pristine $LiNiVO_4$ prepared by the sol-gel (SG) method will be discussed. Few characterizations of the prepared system were implemented for structural, chemical, morphology and electrochemical studies by using the XRD, TGA, SEM, TEM, EDAX, and cyclic voltammetry (CV).

The precursor of the prepared sample was analyzed to determine the suitable calcination temperatures by the TGA. The obtained thermogram result was examined to confirm the chemical mechanism for the $LiNiVO_4$ synthesis by the sol-gel method. The XRD analysis was carried out to confirm the $LiNiVO_4$ crystal structure formation. The SEM and TEM studies were employed to investigate the morphology of the prepared samples by each treated firing temperatures. The EDAX tests surveys on the elemental analysis of the composed samples. The electrochemical study was held by using the cyclic voltammetry (CV) analyzer to study the redox reactions of the fabricated cell using the prepared cathode.

4.2 Structural studies

The XRD study is used to determine the behavior of the crystal structure. Moreover, the XRD data can be used to calculate the crystallite size of the synthesized powder. The crystallite size result will be then compared with the TEM images to relate the theoretical value and the viewing results in the later chapter of the thesis. Moreover, the XRD analysis gives the information to rectify the lattice constants, a and the volumes of crystal cell, V for the mixed doped $LiNiVO_4$ compound. The values obtained were all calculated from the XRD data such as the full- half width maximum (FWHM) and the Bragg's angle of 2-theta at selected *(h k l)* coordination based on the JCPDS data.

4.2.1 X- ray diffraction (XRD)

The $LiNiVO_4$ compounds was synthesized using the starting reactants as explained in the Section 3.2 referred in Table 3.1 on the sample preparations. The obtained pattern shown in Figure 4.1 and clearly depicts that the compound treated at 500 °C is having 2 phases of main product and impurities identified by powder XRD analysis. The small amounts of NiO impurity are present at nearly 37.3°, 43.3° and 62.9° as mentioned in the literature [Fey and Perng, 1997].

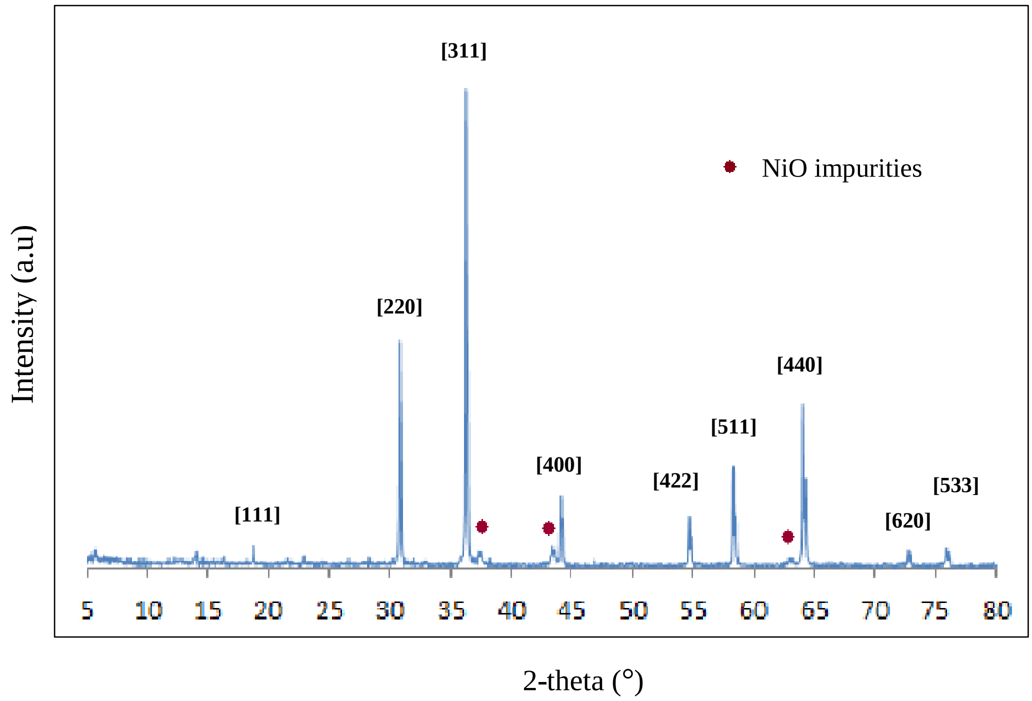

Figure 4.1: Mixed phase for the (LiNiVO$_4$- SG) system at 500 °C

XRD results for the LiNiVO$_4$ synthesized by the sol-gel method are presented in Figure 4.2. The XRD pattern for LiNiVO$_4$ shows that a peak at $2\theta = 18.6°$ at [111] ratio of intensity and the position of [220] peak located at 30.6° confirms the formation of the LiNiVO$_4$ inverse spinel product [Fey and Perng, 1997; Chitra *et. al,* 2000; Kalyani *et. al,* 2002; Subramania *et. al,* 2006]. As we expect, the [220] peak is more intense than the [111] peak for inverse spinel [Fey and Perng, 1997]. The obtained results are in the good agreement with the Joint Committee on Powder Diffraction International Centre for Diffraction Data (JCPDS), 38-1395 for LiNiVO$_4$. The material has shown the phase behaviour for the sample treated at different sintering temperatures.

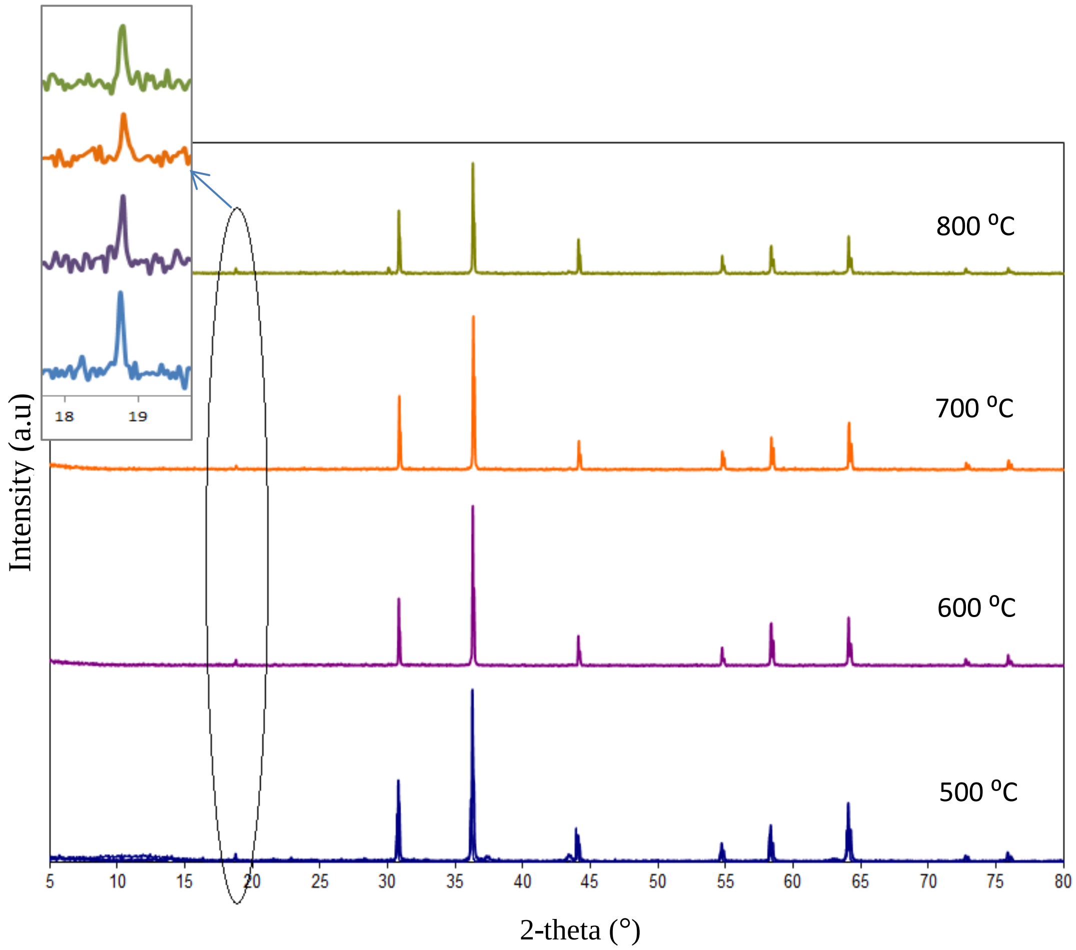

Figure 4.2: XRD pattern for the (LiNiVO$_4$- SG) system

In the other hand, the diffractogram show a single phase of the compound calcined at higher temperature at 600 °C to 800 °C. The calculated intensity ratio of $I_{[220]}/ I_{[311]}$ for single phase of LiNiVO$_4$ is 0.42, 0.49 and 0.57 which show the high crystallinity nature of the compound for sample treated at 600 °C, 700 °C, 800 °C, respectively. The result follows the value reported by Fey et. al, (1994). The value of the lattice constant for the LiNiVO$_4$- SG system was found to be 8.215 Å from the acquired XRD data. The value obtained was in a good agreement with that obtained by JCPDS card for LiNiVO$_4$ where a = 8.220 Å [Card No. 38-1395].

4.2.2 Crystallite size

The crystallite size can be calculated by using XRD data. The XRD data provides pattern information such as full half width maximum (FWHM) value, the space group type, the lattice constants, and the structural system. The obtained XRD pattern can also be compared with the miller indices fitting based on the database. The crystallite size of the powder can be calculated by using the Scherrer equation to calculate the size of each samples obtained from XRD data. The calculation was taken by using broadening peak [311] at $2\theta = 36.2°$ (the strongest peak) of each sample which is mentioned in equation (3.2) on Chapter 3 on the diffraction studies.

Table 4.1 listed the crystallite size of the system, it can be conclude that the particle size is dependent on the thermal properties. The crystallite sizes shown in Table 4.1 above are the calculated value for the average crystal size or the primary size of the powder.

Table 4.1: Crystallite size values for the (LiNiVO$_4$- SG) system

Temperature (°C)	Crystallite Size (nm)
600	68.07
700	42.94
800	66.59

4.3 Chemical Reaction

In this work, the possible reaction steps involved in the preparation of the system will be discussed in this chapter. Based on the observed reaction, when the citric acid was added into the solution, a clear dark purple solution was immediately formed. Subsequently, when the citric acid was added to NH_4VO_3, V_2O_5 is formed [Tsaramyrsi *et. al*, 2001].

$$2NH_4VO_3 + 2C_6H_8O_7 \longrightarrow V_2O_5 + 2\,(NH_4)\,C_6H_7O_7 + H_2O \qquad (4.1)$$

The use of acetates, i.e., $LiCH_3COO$ and Ni $(CH_3COO)_2$, with the citric acid leads to the gas formation of CO_2 (g), as well as H_2O, and a citric acid complex.

$$LiCH_3COO{\cdot}2H_2O + Ni\,(CH_3COO)_2{\cdot}4H_2O + C_6H_8O_7 + 6O_2 \longrightarrow$$
$$LiNiC_6H_5O_7 + 6CO_2 + 12H_2O \qquad (4.2)$$

Tsaramyrsi et. al, (2001) suggested that the V_2O_5 reacts as an oxidant in an acidic solution. Here, the V_2O_5 may be oxidized by $C_6H_8O_7$. The V(V) in V_2O_5 can be reduced to V(IV) with the gas evolution and forms $(VO)^{2+}$ ion. $(NH_4)(VO)\ C_6H_5O_7$ will be produced when the $(VO)^{2+}$ ion was then reacted with $(NH_4)\ C_6H_7O_7$:

$$V_2O_5 + C_6H_8O_7 + 2(NH_4)C_6H_7O_7 + 4O_2 \longrightarrow 2(NH_4)(VO)C_6H_5O_7 + 6CO_2 + 6H_2O \qquad (4.3)$$

Considering all the above reactions from the Eqs. (4.1) to (4.3), the total reaction equation would be as follows:

$$NH_4VO_3 + 2C_6H_8O_7 + LiCH_3COO\cdot 2H_2O + Ni\,(CH_3COO)_2\cdot 4H_2O + 23/2\ O_2 \longrightarrow LiNiC_6H_5O_7 + 2(NH_4)(VO)C_6H_5O_7 + 27/2H_2O + 6CO_2 \qquad (4.4)$$

The total reaction of the dried gel may be composed of $LiNiVO_4\cdot\ (VO)\ (NH_4)\ C_6H_5O_7$, as shown in Eqn. (4.5) in the next thermal studies 4.3 subsection. These products are formed during the continuous heating process and the reaction is further examined by the thermal decomposition process of the prepared precursor by TGA measurement.

4.4 Thermogravimetric Analysis (TGA)

The optimum firing temperature for the precursor was examined by the TGA analysis. The yielded thermogram line by the TGA test was inspected to determine the weight loss for the sample. Therefore, the thermal stability with increasing temperature will be observed.

The TGA and DTGA curves were analysed for the dried precursor in the temperature range from room temperature to 750 °C. The results are shown in Figure 4.3. From the result, the TGA line saturated around 500 °C which tells us that the minimum temperature to sinter the precursor was around 500 °C – 600 °C.

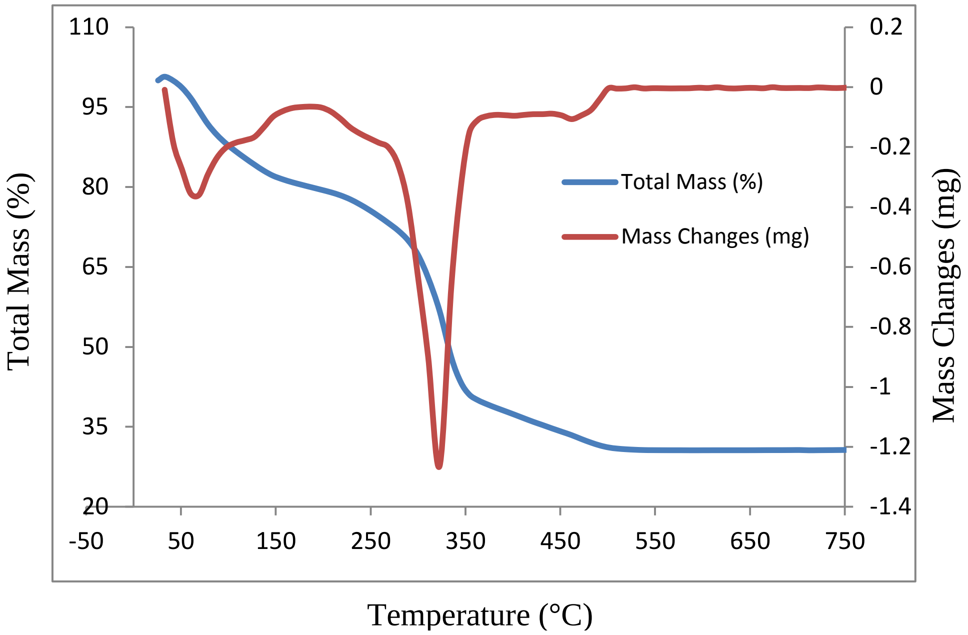

Figure 4.3 TGA and DTGA curve of the LiNiVO$_4$ – SG precursor

The initial weight loss was 10.25 % before 100 °C due to the evaporation of water and decomposition of lithium acetate. In the temperature range from 100 °C to 250 °C, the process complex decomposition of and metal acetates, citric acid and ammonium metavanadate takes place because the melting point for both raw materials are between 100 ºC to 200 °C. The formation of the product goes with two large endothermic peaks in temperature range from 60 °C to 350 °C located separately at 69 °C and 322 °C. Those peaks show a weight loss in the TGA curve. The decomposition process stops at temperature around 500 °C. The total weight loss was 68.76 %. Gasses such as H_2O and CO_2 were gradually reduced. In order to obtain the stable vanadate, the residuals formed will continue to react after the decomposition process. This reaction will cause the weight loss of the compound. The TGA spectra have also been analyzed to elucidate the mechanism for the synthesis of $LiNiVO_4$. The total weight loss of the decomposition process for $LiNiVO_4$ was comparable to the calculated value of 69.5 %, based on the proposed total decomposition equation in air atmosphere:

$$4LiNiC_6H_5O_7{\cdot}(VO){\cdot}\,(NH_4)\,C_6H_5O_7 + 37O_2 \longrightarrow 4LiNiVO_4 + 48CO_2 + 22H_2O + 4NH_3 \qquad (4.5)$$

4.5 Morphology studies

4.5.1 Scanning Electron Microscopy (SEM)

The structural studies in previous chapter already discussed on the crystallinity obtained by the sintered $LiNiVO_4$ at varying temperatures. Here, after the obtained precursor was heated at different sintering temperature using a furnace, the resultants of the treated powders are then left cooled for SEM viewing. Figure 4.4 shows the surface morphology for $LiNiVO_4$- SG system.

The SEM micrograph of $LiNiVO_4$- SG obtained by sintering temperature at 500 ºC for 3 hours is presented in Figure 4.4 (a). The powder obtained shows fluffy morphology and fragile-look particles. Figure 4.4 (b) depicts the powder treated at 600 ºC having less voids. The outline of the particle becomes visibly clearer with the increasing temperature. The obvious particle growth with clear particle edges can be seen in Figure 4.4 (c). The particle clusters of the powder gradually separated, smoother and become more solid. Therefore, the crystallinity of the powder can be observed at higher calcined temperature. Such morphology has been reported [Liu *et. al*, 2002] using carbonates as their starting materials. It was also revealed that the porous morphology for the sample treated at 800 ºC as shown in Figure 4.4 (d).

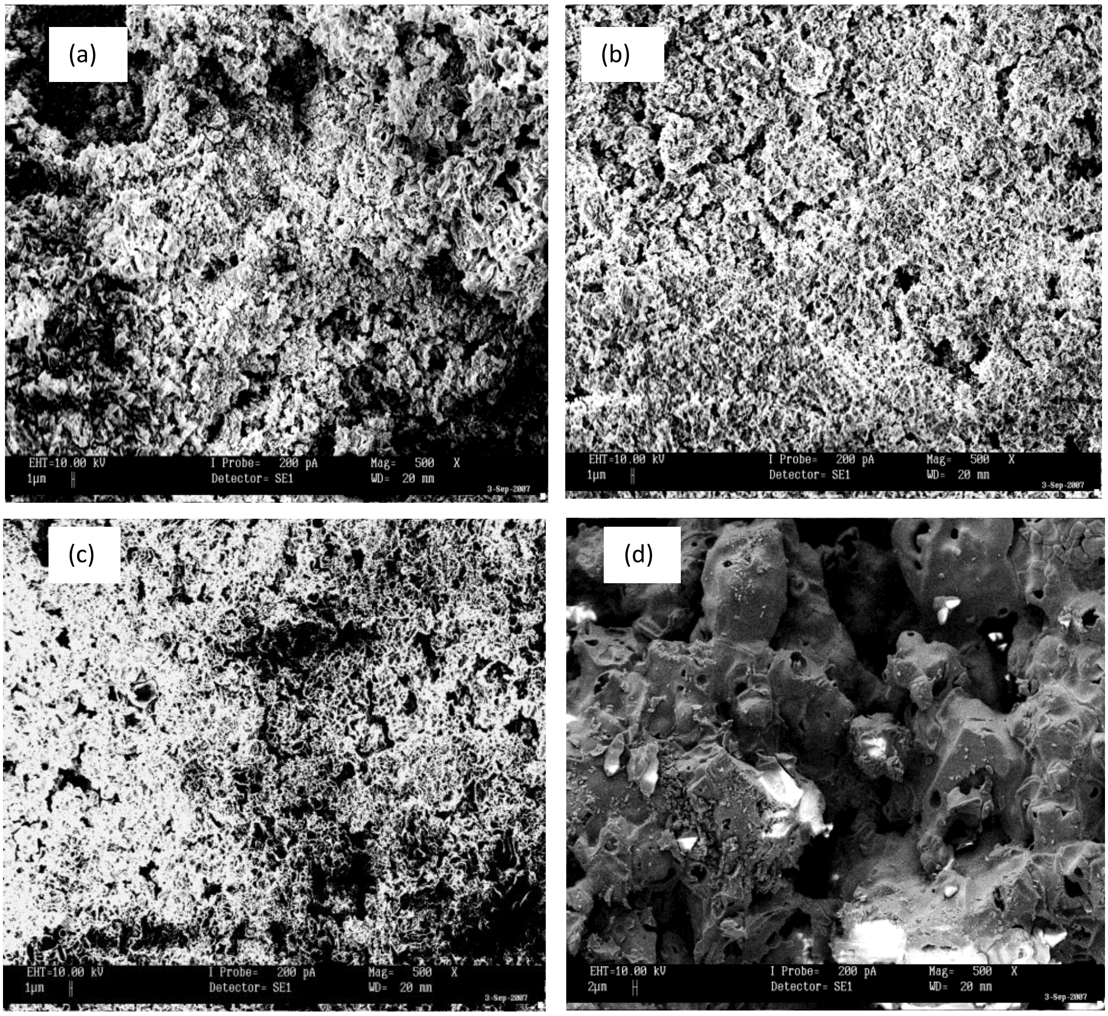

Figure 4.4: Surface morphology of LiNiVO$_4$- SG system (a) LiNiVO$_4$- SG at 500°C; (b) LiNiVO$_4$- SG at 600 °C; (c) LiNiVO$_4$- SG at 700 °C; (d) LiNiVO$_4$- SG at 800 °C with 500X magnification

4.5.2 Transmission Electron Microscope (TEM)

The morphology studies for all system in this work are still not clear if only depends on the SEM results alone since the obtained SEM micrographs display almost the same structure. Therefore, the TEM analysis was done to investigate the detailed morphology of those systems for better understanding on the structure and the particle behavior.

Figure 4.5 depicts the morphology of the LiNiVO$_4$ particle prepared by the sol- gel method.

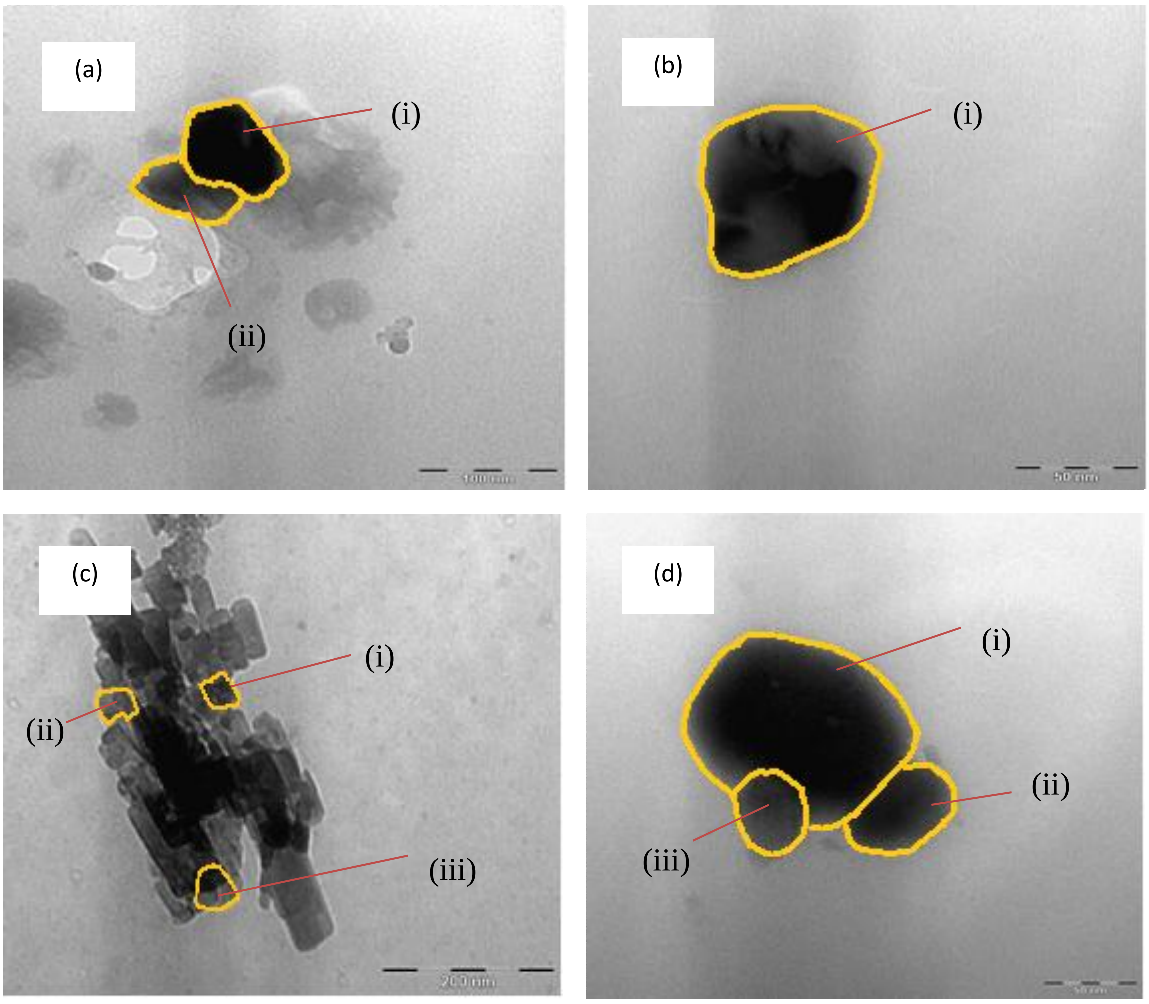

Figure 4.5: TEM images of LiNiVO$_4$- SG system at (a) 500 °C; (b) 600 °C; (c) 700 °C; (d) 800 °C

The single spherical shape for LiNiVO$_4$- SG particle was obtained at lower temperature shown in Figure 4.5 (a and b). The particles marked in Figure 4.5 a (i) and (ii) has 83.0 nm and 77.7 nm, respectively. The particle size of the single spherical shape in Figure 4.5 b (i) is 71.8 nm. As the heating temperature rose up, the particle seems to assemble to each other giving almost the angled shape as demonstrated in Figure 4.5 (c). The particle size in Figure 4.5 c (i) is 44.4 nm. The particles in Figure 4.5 c (ii) and (iii) are having the same size of 53.3 nm. The particles were found to have polyhedral shape as presented in Figure 4.5 (d) at highest heating temperature. Figure 4.5 d (i) depicts particle size of 125 nm while in Figure 4.5 d (ii) and (iii) are 62.5 nm and 16.7 nm respectively. This result is comparable with the crystallite size calculation obtained from the XRD data using Scherrer equation.

4.6 Elemental Studies (EDAX)

The prepared cathode was analyzed by using the Elemental Dispersive X-ray (EDAX) technique with scanning electron microscope (SEM) at accelerating voltage of 20 kV. Bearing in mind for this analyser that lithium, the lightest element is not detected in the measurement due to the limitation of the instrument. The results in Table 4.2 summarized the atomic percentage for LiNiVO$_4$. The obtained data revealed that the Ni and V presence in the elemental measurement.

Table 4.2: Atomic ratio (%) of inverse spinel LiNiVO$_4$ of Ni and V at various sintering temperatures.

	Ni	**V**	**Ni : V**
500 °C	20.44	20.55	1 : 1.0050
600 °C	17.39	20.42	1 : 1.1742
700 °C	15.44	20.95	1 : 1.3569
800 °C	17.19	17.70	1 : 1.0297

Those recorded values for all treated samples shown in Figure 4.6 are close to 1: 1 atomic ratios of Ni: V. No trace of impurities was detected in the analysis. The obtained atomic values and the presence of mentioned elements prove the proportion of the stoichiometric vanadate chemical formula, LiNiVO$_4$. In discussion within ZAF correction for the SEM instruments, the accuracy is about ~ ± 15%. Therefore, the ratio obtained shown in Table 4.2 for each treated sample is about 1: 1.

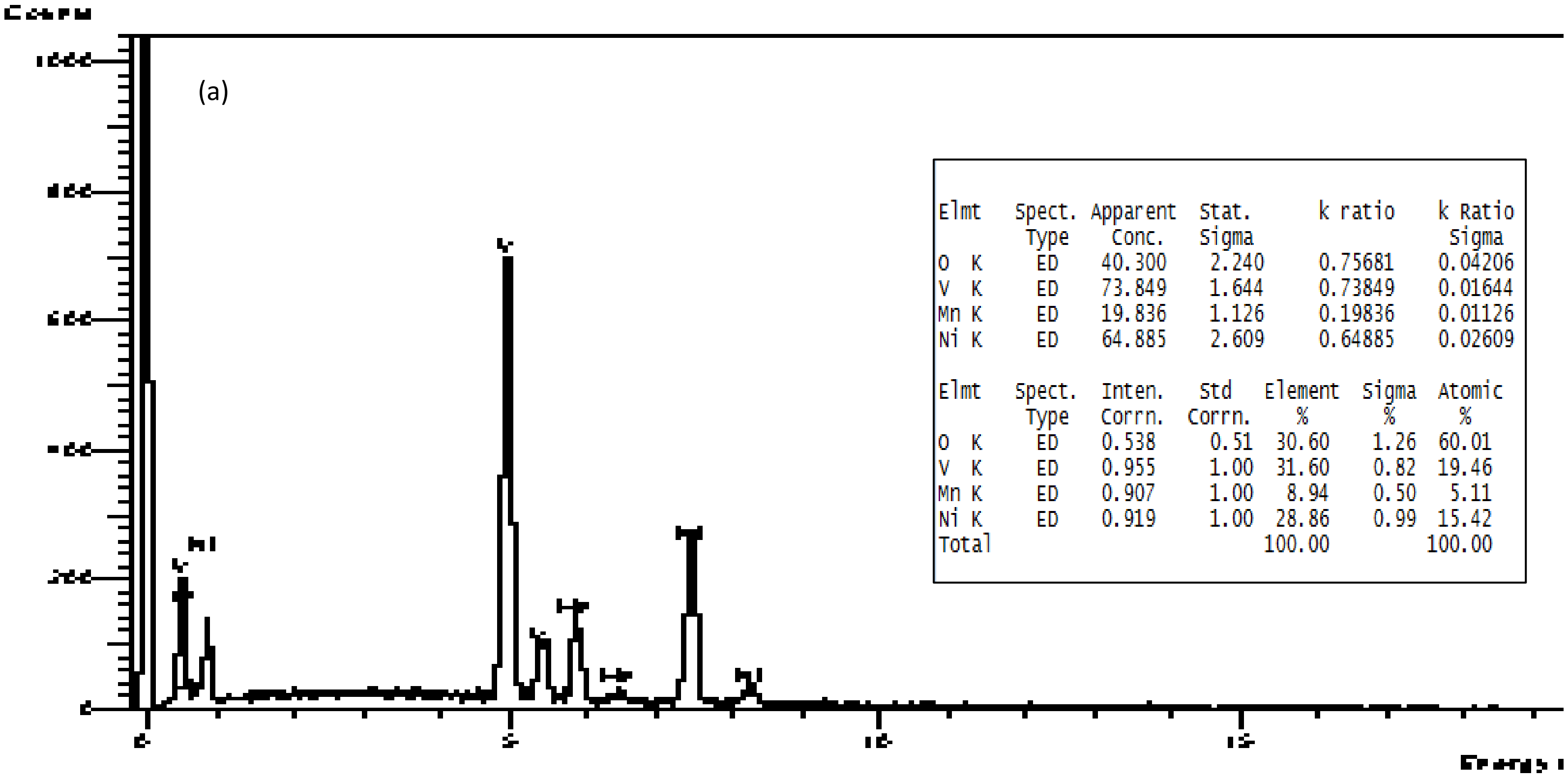

Elmt	Spect. Type	Apparent Conc.	Stat. Sigma	k ratio	k Ratio Sigma
O K	ED	40.300	2.240	0.75681	0.04206
V K	ED	73.849	1.644	0.73849	0.01644
Mn K	ED	19.836	1.126	0.19836	0.01126
Ni K	ED	64.885	2.609	0.64885	0.02609

Elmt	Spect. Type	Inten. Corrn.	Std Corrn.	Element %	Sigma %	Atomic %
O K	ED	0.538	0.51	30.60	1.26	60.01
V K	ED	0.955	1.00	31.60	0.82	19.46
Mn K	ED	0.907	1.00	8.94	0.50	5.11
Ni K	ED	0.919	1.00	28.86	0.99	15.42
Total				100.00		100.00

Figure 4.6 (a): EDAX analysis of the LiNi$_{0.75}$Mn$_{0.25}$VO$_4$ at 500 °C

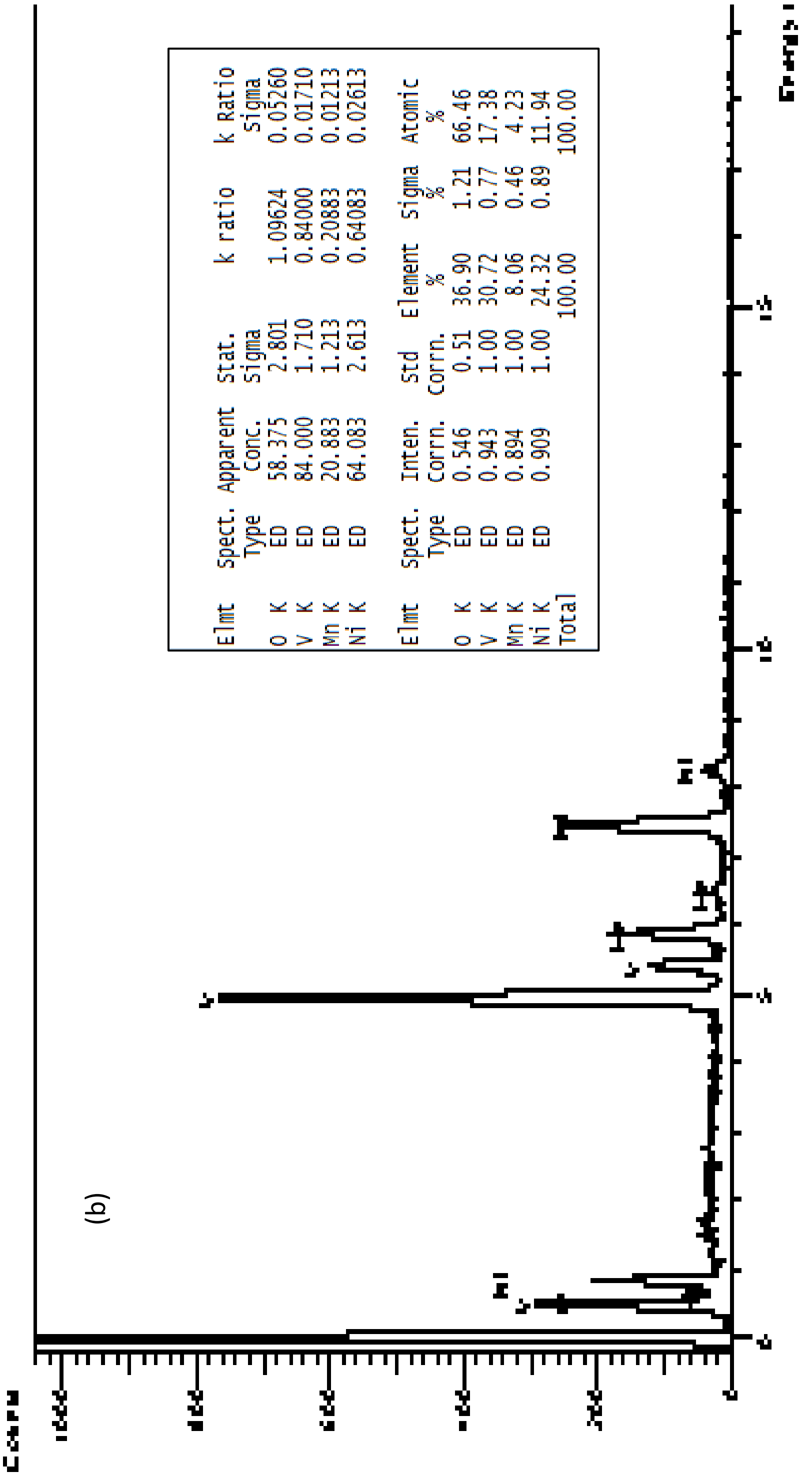

Elmt	Spect. Type	Apparent Conc.	Stat. Sigma	k ratio	k Ratio Sigma
O K	ED	58.375	2.801	1.09624	0.05260
V K	ED	84.000	1.710	0.84000	0.01710
Mn K	ED	20.883	1.213	0.20883	0.01213
Ni K	ED	64.083	2.613	0.64083	0.02613

Elmt	Spect. Type	Inten. Corrn.	Std Corrn.	Element %	Sigma %	Atomic %
O K	ED	0.546	0.51	36.90	1.21	66.46
V K	ED	0.943	1.00	30.72	0.77	17.38
Mn K	ED	0.894	1.00	8.06	0.46	4.23
Ni K	ED	0.909	1.00	24.32	0.89	11.94
Total				100.00		100.00

Figure 4.6 (b): EDAX analysis of the LiNi$_{0.75}$Mn$_{0.25}$VO$_4$ at 600 °C

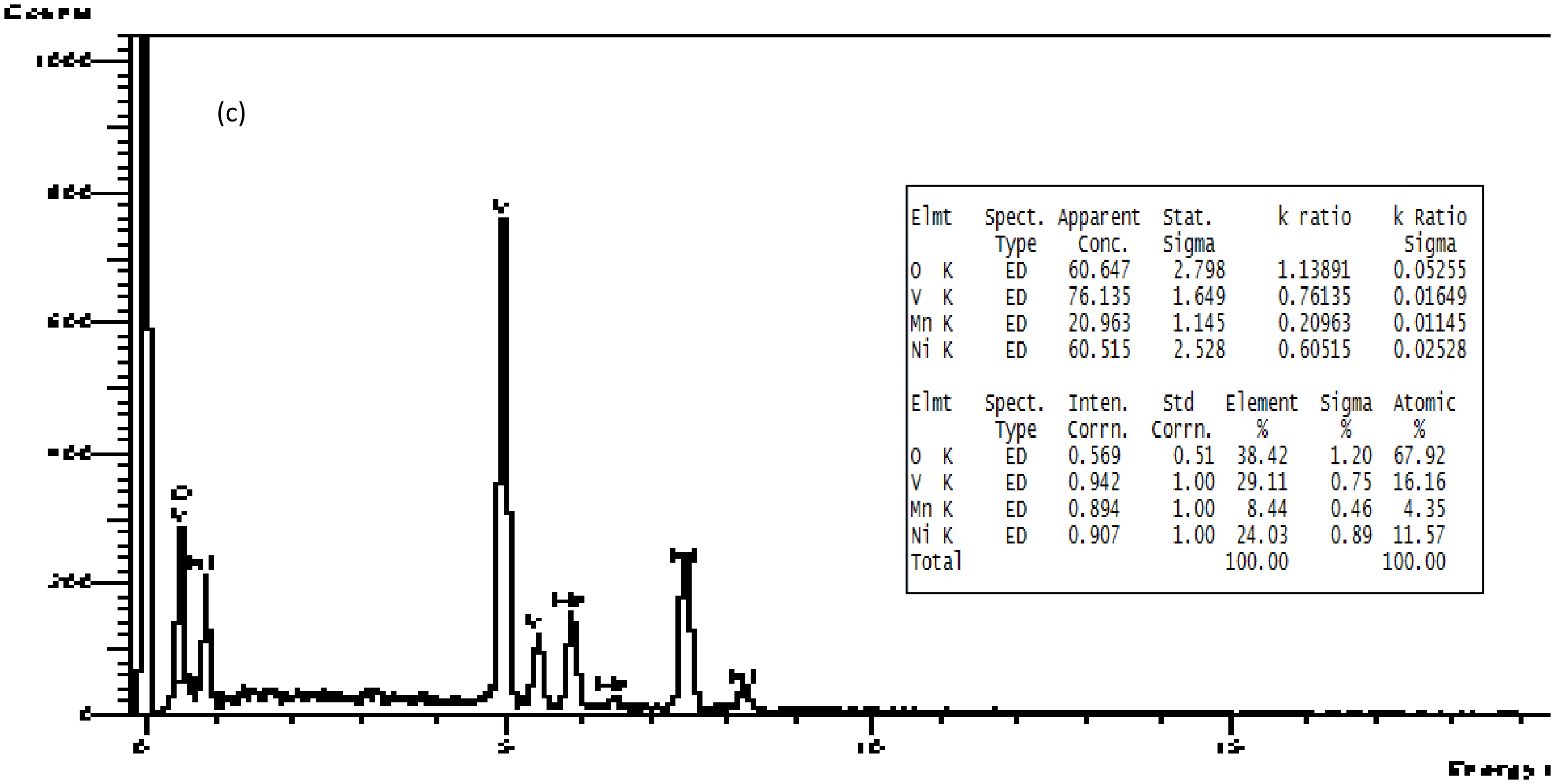

Elmt	Spect. Type	Apparent Conc.	Stat. Sigma	k ratio	k Ratio Sigma
O K	ED	60.647	2.798	1.13891	0.05255
V K	ED	76.135	1.649	0.76135	0.01649
Mn K	ED	20.963	1.145	0.20963	0.01145
Ni K	ED	60.515	2.528	0.60515	0.02528

Elmt	Spect. Type	Inten. Corrn.	Std Corrn.	Element %	Sigma %	Atomic %
O K	ED	0.569	0.51	38.42	1.20	67.92
V K	ED	0.942	1.00	29.11	0.75	16.16
Mn K	ED	0.894	1.00	8.44	0.46	4.35
Ni K	ED	0.907	1.00	24.03	0.89	11.57
Total				100.00		100.00

Figure 4.6 (c): EDAX analysis of the LiNi$_{0.75}$Mn$_{0.25}$VO$_4$ at 700 °C

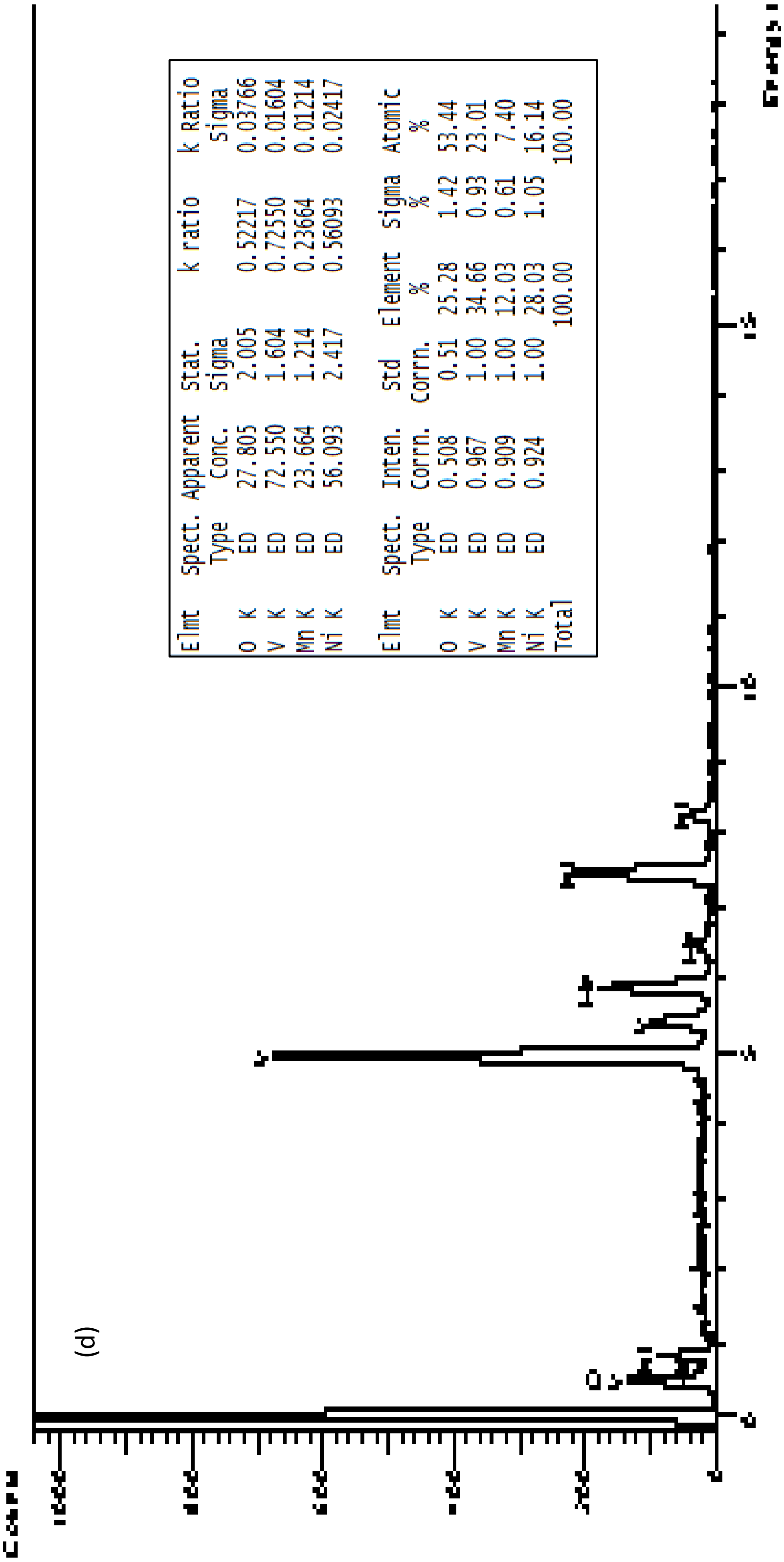

Elmt	Spect. Type	Apparent Conc.	Stat. Sigma	k ratio	k Ratio Sigma
O K	ED	27.805	2.005	0.52217	0.03766
V K	ED	72.550	1.604	0.72550	0.01604
Mn K	ED	23.664	1.214	0.23664	0.01214
Ni K	ED	56.093	2.417	0.56093	0.02417

Elmt	Spect. Type	Inten. Corrn.	Std Corrn.	Element %	Sigma %	Atomic %
O K	ED	0.508	0.51	25.28	1.42	53.44
V K	ED	0.967	1.00	34.66	0.93	23.01
Mn K	ED	0.909	1.00	12.03	0.61	7.40
Ni K	ED	0.924	1.00	28.03	1.05	16.14
Total				100.00		100.00

Figure 4.6 (d): EDAX analysis of the $LiNi_{0.75}Mn_{0.25}VO_4$ at 800 °C

4.7 Cyclic voltammetry (CV)

The cathode material plays an important role of having efficient electrochemical properties in the developed cells. It is also important to make sure the reversibility of chemical species can be achieved at wide potential range. The electrochemical test was performed to analyze the cathode performance by employing cyclic voltammetry (CV) measurement using AUTOLAB software by compatible PC interface. In this work, CV was held to study the Li$^+$ ion kinetics transfer during redox process.

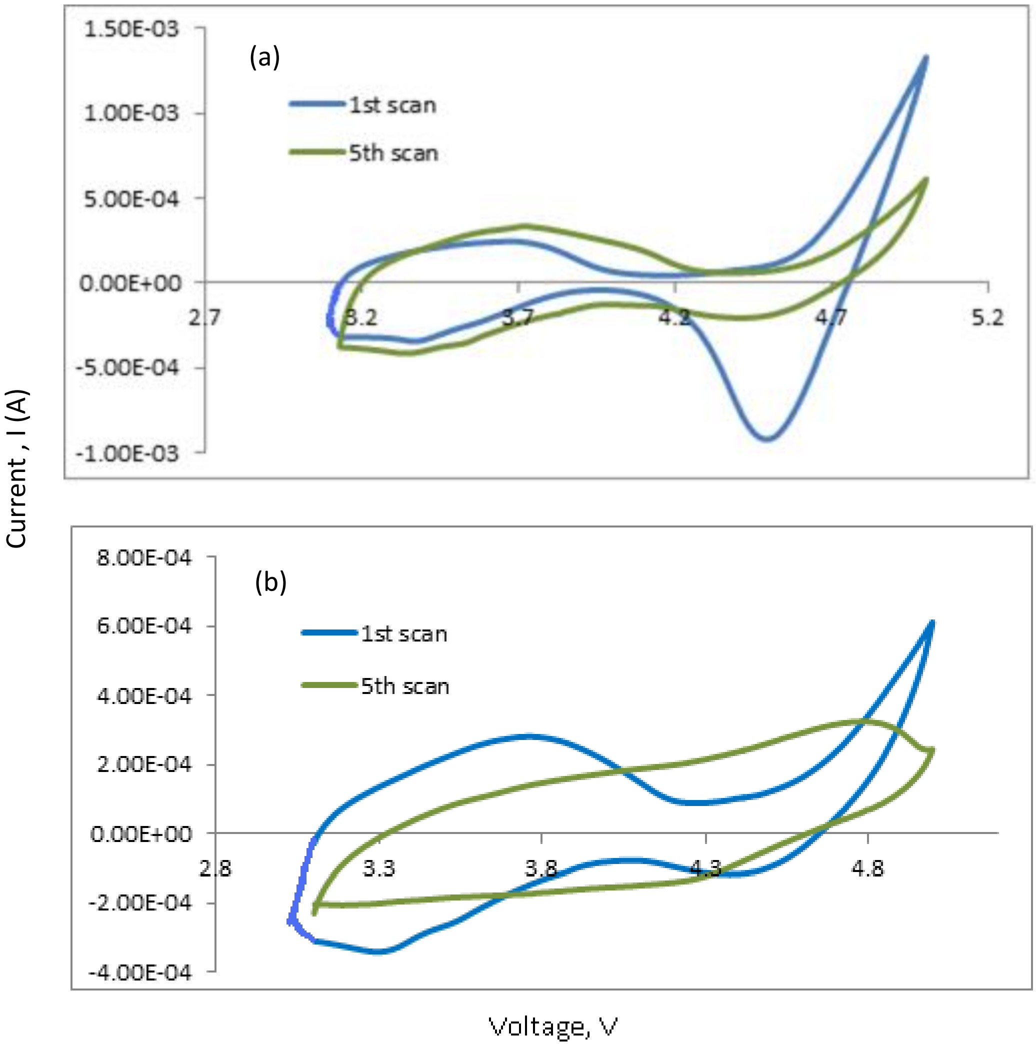

Figure 4.7: Cyclic voltammograms for Li/ LiNiVO$_4$- SG electrode system in 1 mol dm^{-1} LiPF$_6$ in 1:2 by (vol/ vol%) EC/DMC at scan rate of 1 mV/s (a) cathode sintered at 600 °C; (b) cathode sintered at 800 °C

The half- cell was measured at the cell voltage range of 3-5 V. Figure 4.7 shows the cyclic voltammogram of the Li/ LiNiVO$_4$ cell at sweep rate of 1 mV/s at 1st scan and the 5th scan. The voltammogram favor the reversible nature for anodic and cathodic curves for cathode. The anodic curve was observed having a broad and shallow peak at around ~ 3.7 V. The cathodic curves in the electrochemical configuration were large area of cathodic peak at around ~ 4.5 V over few cycling process was obtained. The potential separation between anodic and cathodic peak sintered at lower temperature was about ~ 0.8 V.

The CV features at the 5th scan of the fabricated half- cell using the cathode system behave almost the same pattern having nearly uniform voltage upon cycling especially on the lithium intercalation transfer curve which confirms the reversibility for the Li-de/intercalation. However, the reverse scan on the 5th scan records a slight decrease size on the redox peaks predicts the capacity loss upon cycling. The redox behavior was depicted in Figure 4.7 (b). The anodic peak was at 3.8 V while the cathodic peak was at 4.4 V. Therefore, the potential separation between anodic and cathodic peak of around ~ 0.6 V for the initial scan was acquired at higher sintering temperature. As the cycling number increased to the 5th scan, the voltammogram depicts an improved redox behavior having improved anodic and cathodic peaks at ~ 4.7 V and ~ 4.3 V, respectively as compared to that of shallow anodic peak obtained at lower sintering temperature. However, the redox curve in Figure 4.7 (b) demonstrates the larger area of the redox peak for the active material sintered at higher temperature 800 °C show a better kinetics of the Li$^+$ ion in the cell system.

4.8 Summary

In this work, the pristine $LiNiVO_4$ was successfully synthesized assisted with the citric acid via sol- gel method. The prepared precursor was put in the furnace for various temperature treatments in air for further characterization. The analysis of the fired $LiNiVO_4$ has shown that the formation of the mixed phases including impurities at 500 °C. The result indicated that the single phase of the pure material commence at 600 °C onwards. Based on the XRD data, the calculated crystallite size ranging from the 42.94 nm to 68.07 nm were obtained at firing temperatures for pure $LiNiVO_4$. The reaction mechanism proposed in this work was synonymously in relation with the TGA/ DTGA result. The morphology studies of this work show the growth of the surface of the particle powder upon rising temperature. The presence of porous formation was obtained at the highest firing temperature at 800 °C. Elemental study for the pure $LiNiVO_4$ at all sintering temperatures agrees stoichiometrically with the vanadate formula and the atomic values.

The cyclic voltammetry studies show the redox process with presence of the cathodic and anodic curves that corresponds to the de/ intercalation process of Li- ion. The improved redox was obtained at the highest sintering temperature during the initial scan. This behavior on the CV test suggests better reversibility of the fabricated half- cell for the Li-ion insertion/ extraction.